Rakenteiden Mekaniikka (Journal of Structural Mechanics)
Vol. 57, No. 3, 2024, pp. 126–137
http://rakenteidenmekaniikka.journal.fi
https://doi.org/10.23998/rm.146410

VERTAISARVIOITU
KOLLEGIALT GRANSKAD
PEER-REVIEWED
www.tsv.fi/tunnus

Application of a numerical method in analyzing the operation of single-stage scissor lifts

Anh-Tuan Dang

Summary Scissor lifts are special devices for transporting or lifting with a wide range of applications. By extending or retracting the hydraulic cylinder arranged in the scissor frame, the system can raise or lower the platform to the designated height. This study was conducted to analyze the relationship between the configuration of the cylinder and the movement of the platform in single-stage scissor lifts. By applying a numerical method and assigning parameters for the cylinder arrangement, the displacement of the platform and the forces in the cylinder can be easily calculated. The results obtained from the calculation process show the practicality of the proposed method in determining the optimal configuration for designing single-stage scissor lift systems.

Key words: scissor lift, 2D design, Working Model, dimensional arrangement, cylinder calculation, kinematic analysis

Received: 16 June 2024. Accepted: 5 November 2024. Published online: 5 November 2024.

Introduction

Scissor lifts are lifting devices that use a scissor mechanism to lift or lower goods or people over a short distance. Based on the working requirements of the system, many types of scissor lift systems with different structures and operating methods have been proposed and studied. These differences affect not only the movement of the platform but also the working conditions of the components in the lifts [1, 2].

Numerous studies have been conducted to evaluate the operation of scissor-lift systems. Tian Hongyu [3] utilized Pro/E to evaluate the operation of a four-stage scissor lift system. Although the research is only concerned with the assembly of the components, this is still one of the first studies about designing complex systems in modeling software. Based on calculations from SolidWorks and ANSYS software, Solmazyiğit et al. [4] successfully manufactured a scissor lift with a capacity of up to 25 tons. The study also proposed several special structures to ensure system safety during manufacturing, such as the hinge system, bushing bearing, and guiding frames. Görkem

Dengiz et al. [5] SolidWorks to determine the change of reactions on pivot joints according to the platform elevation in a double-layer scissor lift. Karagülle et al. [6] created an assembly model of a double-stage scissor lift system in SolidWorks to determine internal loads on component frames and evaluate system rigidity and dynamic stability.

Although 3D modeling to analyze complex systems can effectively support the design process, building a model with specific dimensions consumes considerable time. Even minor changes in the structure can affect the entire process, which sometimes requires redesigning all related components before proceeding with the simulation. Therefore, another approach proposed for designing scissor lift systems is to use general mathematical expressions to describe the kinematic and dynamic relationships of the components in the system, thereby shortening the design and analysis time. Spackman [7] used simple mathematical expressions to analyze the mechanism of scissor lifts. The study not only analyzed reactions in the members but also presented issues related to the placement of the cylinder and the strength of the component links. To calculate longitudinal and flexural deflection in cantilevers of n-stage scissor systems, Kirsanov [8] proposed a set of formulas that consider the cross-section shapes and material of component frames. In addressing static problems of scissor lift systems, Dang et al. [9, 10] suggested a parametric method for different configurations of double-stage scissor systems. Todorović et al. [11] applied Harris Hawks Optimization (HHO) to reduce mass in the mechanism frames. The study paper proposes a derivation for a general force expression, in terms of a few carefully chosen position variables, which can generate the force expression for any actuator position. Saxena [12] derived an n-stage scissor lift system to obtain the relationship between the cylinder thrust and the load on the platform as a function of velocities. The results from the study showed that the proposed method can be used for the analysis of not only the output force but also the ratio of velocities between component links. Čuchor et al. [13] solved static equations in single-layer structures to calculate the force in the cylinder. Expressions acquired from the calculation assist the construction of lifting loads with a capability of up to 3.5 tons. Cornel Ciupan [14] proposed an algorithm to calculate the double-stage scissor-lift systems based on the dimension of the component link. A Mathcad program was developed to determine the detailed data, including the number of scissor frames with dimensions and forces in the pivot joints. However, due to the diversity of cylinder structures, some configurations have not been fully analyzed, and most up-to-date commercial lifting systems are constructed based on experience or experimental models.

This study analyzes the operation of a specific type of scissor lift, as depicted in Figure 1. By applying algebraic methods to solve position equations, the relationship between the cylinder arrangement and platform movement is determined and presented in instructional diagrams. The study also proposes an expression that relates the arrangement parameters, the thrust force on the cylinder, and the forces at the pin joints. Using these results, the bending moment diagrams of the member frames are also calculated, which can serve as a guide for designing the entire system.

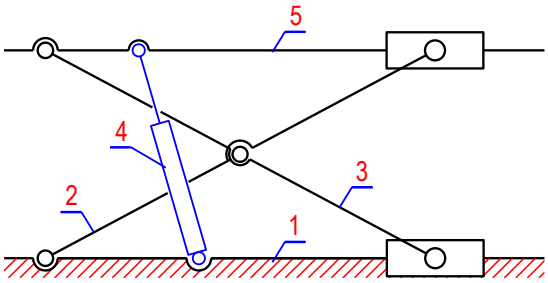

Figure 1. Structure of the system: 1. Ground frame, 2. Rotated frame, 3. Planar frame, 4. Cylinder, 5. Platform.

Kinematic analysis

Analyzing the operation of the system in Figure 1 indicates that the platform raises when the cylinder extends and lowers when the cylinder retracts. Depending on the orientation of the cylinder, specifically the positions of P and Q, the height H of the platform might vary even when the same cylinder is used. Therefore, it is difficult for designers to choose the exact configuration for the system to simulate the system's movement.

Assigning parameters as AB = CD = L, DQ = αL, AP = βL, and PQ = λL (with $\lambda > 0$ and $1 > \alpha, \beta > 0$), the complex dimension system can be transformed into one with basic parameters α, β, and λ, using a scaling ratio of frame length L, as presented in Figure 2. For a system using a cylinder with given dimensions (the maximum and minimum lengths of PQ, or λ_{max} and λ_{min}), analyzing the system's operation involves evaluating the positions of component links and joints according to the cylinder's movement.

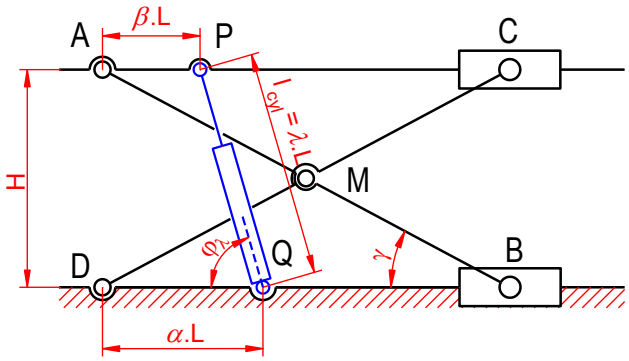

Figure 2. Assign parameter for the system's dimensions.

During the cylinder's extension, the platform raises to an elevation H above the ground, which can be represented by the following expressions:

$$H = \sqrt{l_{cyl}^2 - (\mathrm{DQ} - \mathrm{AP})^2} = L\sqrt{\lambda^2 - (\alpha - \beta)^2} \quad (1)$$

It means that during the extension of the cylinder from $l_{cyl.min} = L.\lambda_{\min}$ to $l_{cyl.max} = L.\lambda_{\max}$ the platform raise its height from $H_{\min}$ to $H_{\max}$ with a displacement ratio k_H:

$$k_H = \frac{H_{\max} - H_{\min}}{L} = \left[\sqrt{\lambda_{\max}^2 - (\alpha - \beta)^2} - \sqrt{\lambda_{\min}^2 - (\alpha - \beta)^2} \right] \quad (2)$$

Based on this equation, the orientation of cylinder can also be determined as:

$$|\alpha - \beta| = \sqrt{\lambda_{\max}^2 - \left(\frac{k_H^2 + \lambda_{\max}^2 - \lambda_{\min}^2}{2k_H} \right)^2} \quad (3)$$

To illustrate, for a lifting system with 150-cm frame length (L = 150cm), using a cylinder with an initial length $l_{cyl.min}$ = 60 cm and 45-cm stroke (λ_{min} = 0.4 and λ_{max} = 0.7), if the requirement raising height is 60 cm (k_H = 0.4), the orientation of the cylinder can be determined as

$$|\alpha - \beta| = \sqrt{0.7^2 - \left(\frac{0.4^2 + 0.7^2 - 0.4^2}{2 \times 0.4} \right)^2} = 0.339$$

This means that the arrangement coefficients of α = 0.4 and β = 0.739 or β = 0.061, corresponding to AP = αL = 0.4×150 = 60 cm and BQ = 110.85 cm or BQ = 9.15 cm, can be chosen to meet the requirement.

Figure 3 describing a basic instruction for the selection of cylinder according to the cylinder orientation (α - β) and working range of the platform (H/L):

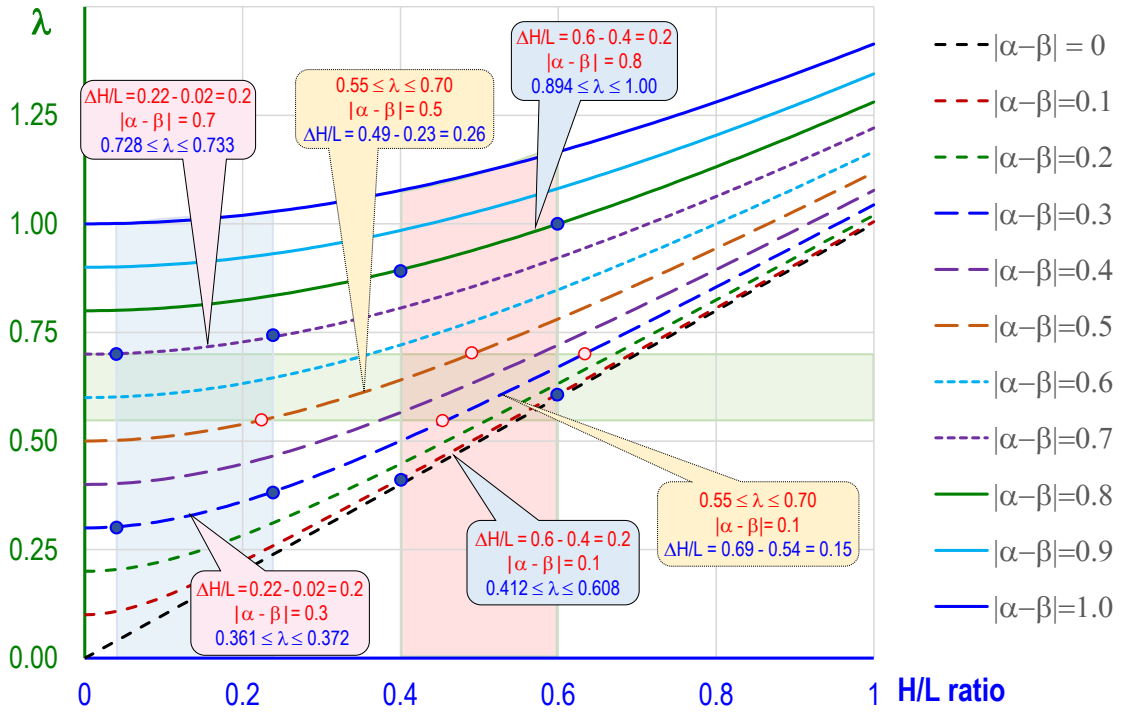

Figure 3. Working range of the angle frame γ with variable of (α - β) and λ

According to the figure, the design factors of the system (including selecting the appropriate cylinder and its arrangement in the lift) can be chosen as follows: Assume

designers must choose a cylinder to be arranged in a given scissor lift with a frame length of L = 1 m to achieve a required platform displacement of 0.2 m. First, the displacement range of the system must be $(H_{max} - H_{min})/L = 0.2$, meaning the working range of the system must be within the colored region presented in Figure 3. Based on the position of the pin joints for assembling the cylinder (represented by β and α, specifically the value of $|\alpha - \beta|$), the detailed dimensions of the cylinder can be selected. For the given displacement range of H_{min} = 0.02 m and H_{max} = 0.22 m, designers can choose a cylinder with 0.728 m initial length, 0.733−0.728 = 0.05 m stroke, and arrange positions that (α - β) L = 0.7 m. Alternatively, designers can select a cylinder with an initial length of 0.361 m and a 0.011 m stroke to be arranged in a position where (α - β) L = 0.3 m, to achieve the same displacement range for the platform. For another case with H_{min} = 0.4 m and H_{max} = 0.6 m (to acquire the same displacement range of 0.2 m), designers can select a cylinder with an initial length of 0.894 m and a 0.106 m stroke, using cylinder arrangement parameters of α = 0.1 and β = 0.9. Alternatively, a cylinder with an initial length of 0.412 m, and 0.196-m stroke with arrangement parameters of α = 0.4 and β = 0.3 can be selected to have the same results.

The diagram also indicates that when using the same cylinder, the lifting stroke varies depending on the arrangement of the assembly joint for the cylinder. For example, if a cylinder with an initial length of 0.55 m and a 0.15 m stroke is assembled with arrangement parameters of α = 0.4 and β = 0.3, the system's operating range will be ΔH/L = 0.49 − 0.23 = 0.26 m. However, if the arrangement parameters are α = 0.8 and β = 0.3, the platform will move with a smaller displacement ΔH/L = 0.69 − 0.54 = 0.15 m.

Kinetic analysis

During the operation of the system, the magnitude and direction of forces at pivot joints vary. For the given load $\mathbf{P_G}$ located at point G on the platform, as illustrated in Figure 4, at the lowest position of the platform, the load is positioned at hinges A, P, and C. However, as the platform raises, support C moves closer to A while the distance between A and G remains unchanged. This change affects the balancing of the structure and alters the magnitude of forces acting on the frames.

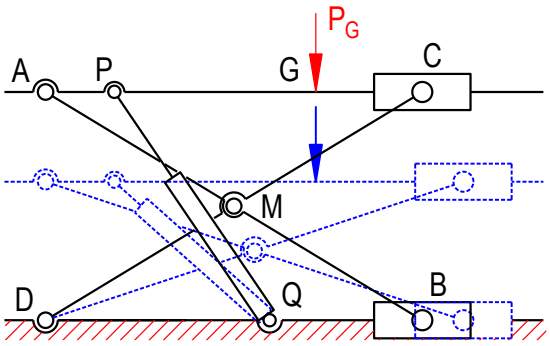

Figure 4. Position of load P_G during the operation of the system

Assuming the distance from loading point G to point A is constant, Figure 5 presents the free-body diagram of the component links after releasing the connection at the revolute joint in the system.

Given that the system operates in a 3D environment while the analysis is conducted in a 2D model, the results of the calculation will be distributed based on the real system's setup, which takes into account variables such as the number of cylinders and scissor frames. By assuming that the platform moves at a slow enough pace to minimize the influence of velocity or acceleration (for disregarding the effects of inertia), and by assuming that the ` of the frames in the system is insignificant, the analysis of the load P_G's impact on the pin joints can be conducted under static conditions.

If the position of the loading point G is fixed (l_P = constant), the free-body diagram of the component links after disconnecting the connection at the revolute joint can be depicted, as presented in Figure 5.

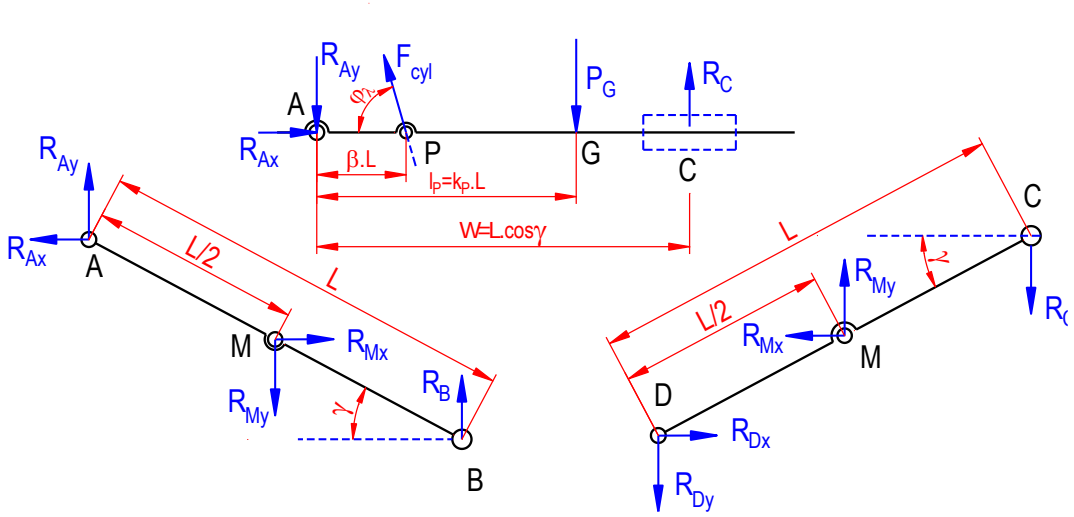

Figure 5. The free-body diagram of scissor frames AD, BC and platform AC

where $\mathbf{F}_{cyl}$ represents the reaction of the cylinder along its axis; $\mathbf{R}_B$ and $\mathbf{R}_C$ denotes reactions on the translating joints, perpendicular to the frames. To simplify the calculation process, the reactions at points A, D and M are decomposed into axial direction components.

Using the equations of force and moment equilibrium for frame AB:

$$\Sigma \mathbf{F}_x = \mathbf{R}_{Ax} + \mathbf{R}_{Mx} = 0 \tag{4}$$

or

$$-\mathbf{R}_{Ax} = \mathbf{R}_{Mx} \tag{5}$$

$$\mathbf{M}_B = -\mathbf{R}_{Mx}.\frac{L}{2}\sin\gamma + \mathbf{R}_{My}.\frac{L}{2}\cos\gamma + \mathbf{R}_{Ax}.L\sin\gamma - \mathbf{R}_{Ay}.L\cos\gamma = 0 \tag{6}$$

Substitute equation (5) into equation (6):

$$\mathbf{R}_{Mx}.\frac{L}{2}\sin\gamma + \mathbf{R}_{My}.\frac{L}{2}\cos\gamma = \mathbf{R}_{Ay}.L\cos\gamma \tag{7}$$

Using equations of moment equilibrium for frame CD:

$$\mathbf{M}_D = \mathbf{R}_{Mx}.\frac{L}{2}\sin\gamma + \mathbf{R}_{My}.\frac{L}{2}\cos\gamma - \mathbf{R}_C.L\cos\gamma = 0 \quad (8)$$

Based on equations (7) and (8), the reactions $\mathbf{R}_{Ay}$ and $\mathbf{R}_C$ can be represented as:

$$\mathbf{R}_{Ay} = \mathbf{R}_C = \frac{\mathbf{R}_{Mx}\tan\gamma + \mathbf{R}_{My}}{2} \quad (9)$$

Using equations of force equilibrium for platform AC:

$$\Sigma\mathbf{F}_x = \mathbf{R}_{Ax} + \mathbf{F}_{cyl.x} = 0 \quad (10)$$

or
$$\mathbf{R}_{Ax} = -\mathbf{F}_{cyl.\mathrm{x}} = \mathbf{F}_{cyl}.\cos\varphi_\lambda \quad (11)$$

Using equations of moment equilibrium for platform AC:

$$\mathbf{M}_P = \mathbf{R}_{Ay}.L\beta - \mathbf{P}_G.\left(Lk_P - L\beta\right) + \mathbf{R}_C\left(L\cos\gamma - L\beta\right) = 0 \quad (12)$$

and
$$\mathbf{M}_A = \mathbf{F}_{cyl}\sin\theta_\lambda.L\beta - \mathbf{P}_G.Lk_P + \mathbf{R}_C.L\cos\gamma = 0 \quad (13)$$

Substitute equation (9) into equation (12):

$$\mathbf{R}_C\cos\gamma = \mathbf{P}_G\left(k_P - \beta\right) \quad (14)$$

Substitute equation (14) into equation (13):

$$\mathbf{F}_{cyl} = \frac{\mathbf{P}_G}{\sin\theta_\lambda} = \frac{\mathbf{P}_G L\lambda}{H} = \frac{\mathbf{P}_G\lambda}{\sqrt{\lambda^2 - \left(\alpha-\beta\right)^2}} \quad (15)$$

In this equation, the force application factor k_P is omitted, indicating that the position of the load $\mathbf{P}_\mathrm{G}$ on the platform does not affect the magnitude of the cylinder thrust force $\mathbf{F}_{cyl}$. On the other hand, the equation also points out that the larger the difference in cylinder orientation $|\alpha\text{-}\beta|$, the higher the required thrust force for the cylinder to operate the lift.

Reactions on the remaining joints are obtained by substituting equation (15) into the other equations, as follows:

$$\mathbf{R}_{Ax} = \mathbf{R}_{Mx} = \mathbf{R}_{Dx} = \mathbf{F}_{cyl}.\cos\varphi_\lambda = \frac{\mathbf{P}_G\left(\alpha-\beta\right)}{\sqrt{\lambda^2 - \left(\alpha-\beta\right)^2}} \quad (16)$$

$$\mathbf{R}_C = \mathbf{R}_{Ay} = \frac{\mathbf{P}_G\left(k_P-\beta\right)}{\sqrt{\left(\alpha-\beta\right)^2 + 1 - \lambda^2}} \quad (17)$$

$$\mathbf{R}_{My} = 2\mathbf{R}_{Ay} - \mathbf{R}_{Ax}\tan\gamma = \frac{\mathbf{P}_G\left(2k_P-\alpha-\beta\right)}{\sqrt{1+\left(\alpha-\beta\right)^2 - \lambda^2}} \quad (18)$$

$$\mathbf{R}_B = \mathbf{R}_{Dy} = \mathbf{R}_{My} - \mathbf{R}_{Ay} = \frac{\mathbf{P}_G\left(k_P-\alpha\right)}{\sqrt{1+\left(\alpha-\beta\right)^2 - \lambda^2}} \quad (19)$$

To evaluate the accuracy of the calculated equations, a simulation model was constructed using Working Model software. By applying a force $\mathbf{P}_G$ to the platform AC, the reactions at the component joints were measured, as shown in Figure 6. The results from the simulation process were compared with those obtained by applying the numerical method and are summarized in Table 1. $\mathrm{F_{WM}}$ is the reaction at joints acquired

from the Working Model software; F_{cal} are results obtained by using the numerical equations (18)–(22) and $\Delta = \left|\frac{F_{cal} - F_{WM}}{F_{cal}}\right| .100\%$ is the difference between the two methods.

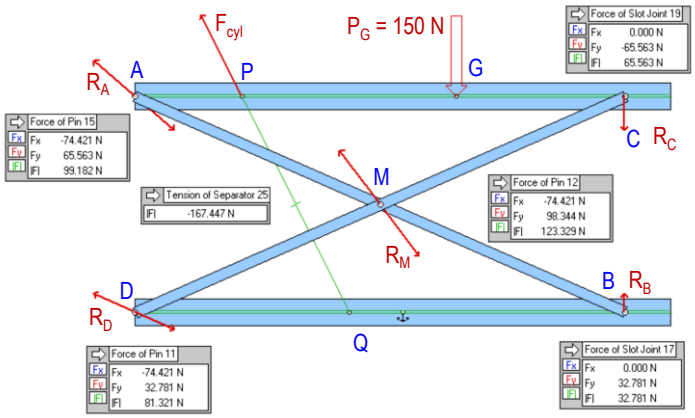

Figure 6. Using the Working Model software to measure reactions on joints

Table 1. Comparing reactions between the calculation method and the simulation model

L = 1.00 m P_G = 500 N		α = 0.20; β = 0.40; l_G = 0.35				α = 0.40; β = 0.10; l_G = 0.80			
		F_{cyl}	F_{Ax}	F_{Ay}	F_{My}	F_{cyl}	F_{Ax}	F_{Ay}	F_{My}
λ = 0.33	F_{WM} (N)	628.60	380.97	25.91	51.82	1200.15	1091.04	353.36	555.273
	F_{cal} (N)	628.60	380.97	25.91	51.82	1200.20	1091.09	353.36	555.27
	Δ%	0.00	0.00	0.00	0.00	0.00	0.00	0.00	0.00
λ = 0.45	F_{WM} (N)	558.24	248.25	27.31	54.63	670.51	446.85	371.54	583.94
	F_{cal} (N)	558.16	248.07	27.32	54.64	670.82	447.21	371.52	583.82
	Δ%	0.01	0.07	0.04	0.02	0.05	0.08	0.01	0.02
λ = 0.72	F_{WM} (N)	520.48	144.58	34.62	69.23	550.02	229.18	462.94	727.47
	F_{cal} (N)	520.48	144.58	34.62	69.23	550.02	229.17	462.94	727.47
	Δ%	0.00	0.00	0.00	0.00	0.00	0.00	0.00	0.00

The results in Table 1 demonstrate the precision of the numerical approach in determining the magnitude of reactions within the system, with a slight variance of less than 0.08%, possibly due to the initial settings from the software. Moreover, these findings indicate that based on the given information, reactions at every joint of the system can be accurately calculated without constructing or simulating on complex 3D models.

The acquired equations not only facilitate the process of determining loads at the joints for bearing design but also aid in selecting a suitable cylinder for the system. For

instance, consider a system with a frame length of L = 1 m and given cylinder arrangement parameters of α = 0.2 and β = 0.35. By applying equation (4), the feasible cylinder coefficient λ is determined, ranging from 0.15 to 0.95. If the required platform displacement is 20 cm (corresponding to k_H = 0.20), and the cargo is placed at G with $\mathbf{P}_G$ = 500N and k_P = 0.35, Figure 7 illustrates the results of the calculation using the given parameters, and Table 2 presents an example for the selection of cylinders and bearings in the revolute joints (A, D, and M) for the system based on the figure.

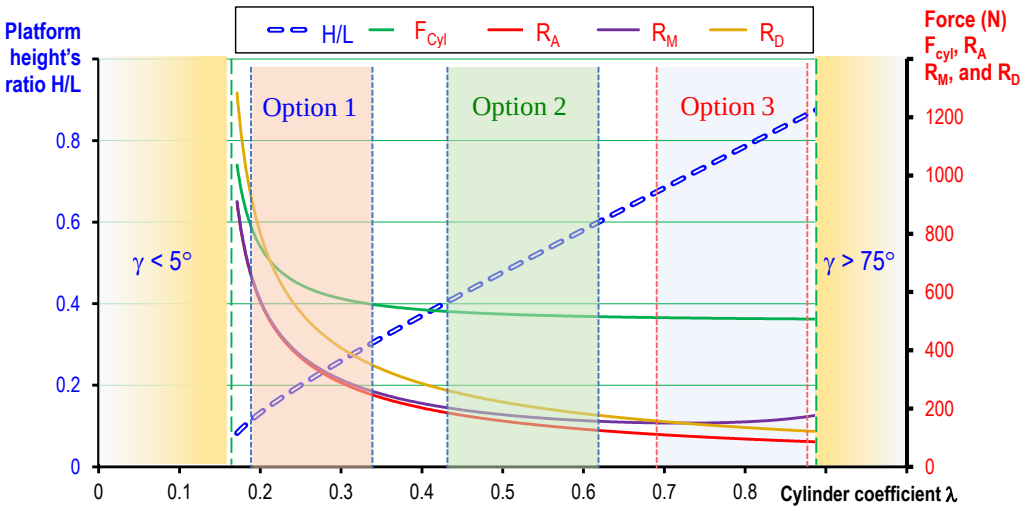

Figure 7. Using the numerical approach to select appropriate cylinders for the system (α = 0.2; β = 0.35; $\mathbf{P}_G$ = 500N; k_P = 0.35; 5° < γ < 75°)

Table 2. The three options selected from Figure 7 have a displacement coefficient k_H = 0.2

	Option 1		Option 2		Option 3	
Position	Lowest	Highest	Lowest	Highest	Lowest	Highest
H/L	0.12	0.32	0.40	0.60	0.67	0.87
λ	0.19	0.36	0.43	0.62	0.69	0.88
$\mathbf{F}_{cyl}$ (N)	797.77	549.38	533.95	515.44	512.39	507.38
$\mathbf{R}_A$ (N)	621.64	227.65	187.35	125.21	112.00	86.24
$\mathbf{R}_M$ (N)	626.21	241.11	204.45	156.36	150.80	174.70
$\mathbf{R}_D$ (N)	879.13	321.94	264.95	177.07	158.39	121.96

The results in Table 2 show that as the platform lifts higher, the load on the component joints decreases, making it easier to select cylinders with a reasonable working range and suitable loads. For instance, option 1 suggests a heavy-duty cylinder with a 19-cm initial length, a 17-cm stroke, and a capable load of 800 N. On the other hand, the other options propose using longer cylinders with smaller loads (less than 550 N): one with an initial length of 43 cm and another with an initial length of 69 cm (both

have the same stroke of 19 cm). The table also shows that the bearing load at joints A, M, and D in option 1 is significantly higher than in the other two options. However, it is important for designers to consider that as the platform rises, the angle γ between the two scissor arms increases, which reduces the stability of scissor systems. Therefore, when evaluating the operational effectiveness of the system, and comparing data from options 2 and 3, although the differences in cylinder thrust force are quite similar and reaction forces at the pin joints is larger, Option 2 is generally preferred.

Based on the calculated equations, the loading state of each frame can also be analyzed, allowing for the determination of whether the structure is in a bending or tensile/compressive state. For example:

1. By projecting reactions on joints B and D perpendicular to the scissor frames AB and CD, the new forces $R'_C = R_C \sin\gamma = P_G\left(k_P - \beta\right)$ and $R'_B = R_B \sin\gamma = P_G\left(k_P - \alpha\right)$ are obtained. If the loading coefficient k_P is fixed, then these forces will create constant bending moment for the two frames in every position of the system.

2. By applying equilibrium equations for the component link (scissor frame and platform), the bending moment in each member can be expressed. This facilitates the selection of appropriate material or cross-section for these structures.

Regarding to the problem, Figure 8 presents the bending moment diagram for the component frame:

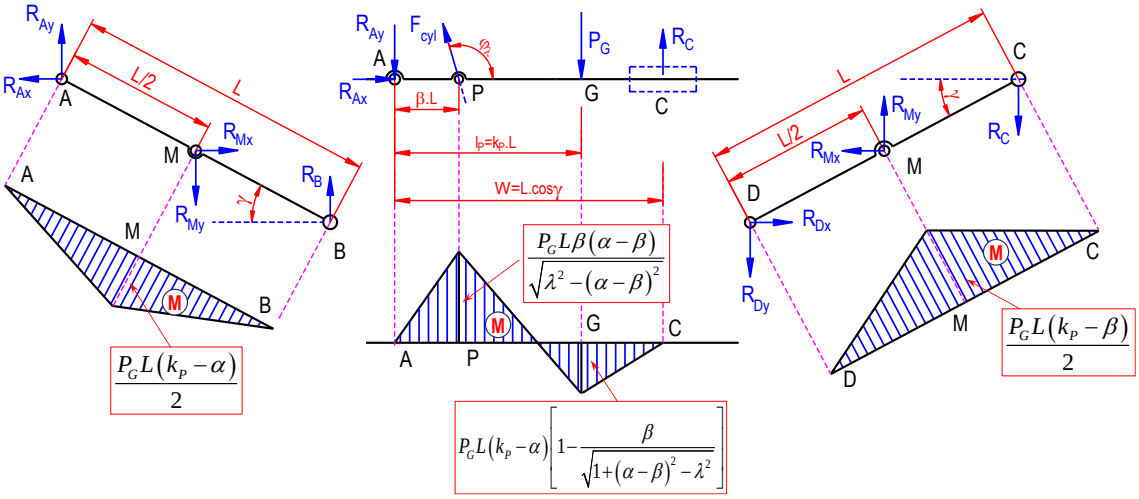

Figure 8. Bending moment M and diagrams in the component frames

Conclusions

The study examines the feasibility of a numerical approach utilizing variables in designing lifting mechanisms employing scissor mechanisms. Three main conclusions emerge from the study:

1. The study presents using numerical methods for analyzing the operation of a 1x scissor lift, demonstrating the feasibility of calculate the kinematic and dynamic parameters solely from the configuration of the system. The results show relationships for lifting load and platform height as functions of cylinder parameters and positioning. With a difference of less than 0.08% compared to simulation software, the proposed method is verified, simplifying the calculation process and removing the need for complex 3D models.

2. Based on the resulting equations, this approach offers solutions for various challenges, including: Calculating platform displacement based on cylinder positioning and range; Determining cylinder thrust load and optimal mounting positions to maximize lift capacity at a given height; and Assessing load distribution at joints and the maximum bending moment on the scissor frame. These solutions facilitate selecting suitable components, such as bearings, frame materials, cross sections, and cylinder specifications.

Acknowledgement

A special thanks to the Thai Nguyen University of Technology for funding this research.

References

[1] C. S. Pan, S. S. Chiou, T. Y. Kau, B. M. Wimer, X. Ning, P. Keane. Evaluation of postural sway and impact forces during ingress and egress of scissor lifts at elevations. *Applied Ergonomics*, 65:152–162, 2017. http://dx.doi.org/10.1016/j.apergo.2017.06.009

[2] V. Paramasivam, S. Tilahun, A. Kerebih Jembere, S. K. Selvaraj. Analytical investigation of hydraulic scissor lift for modular industrial plants in Ethiopia. *Materials Today: Proceedings*, 46:7596–7601, 2021. http://dx.doi.org/10.1016/j.matpr.2021.01.838

[3] T. Hongyu, Z. Ziyi, Design and Simulation Based on Pro/E for a Hydraulic Lift Platform in Scissors Type. *Procedia Engineering*, 16:772–781, 2011. http://dx.doi.org/10.1016/j.proeng.2011.08.1153

[4] İ. Solmazyiğit, R. C. Başkurt, İ. Ovalı, E. Tan, Design and Prototype Production of Scissor Lift Platform 25 Tons Capacity. *The European Journal of Research and Development*, 2:326–337, 2022. http://dx.doi.org/10.56038/ejrnd.v2i4.177

[5] C. Görkem Dengiz, M. Can Şenel, K. Yıldızlı, E. ve Koç. Design and Analysis of Scissor Lifting System by Using Finite Elements Method. *Universal Journal of Materials Science*, 6:58–63, 2018. http://dx.doi.org/10.13189/ujms.2018.060202

[6] H. Karagülle, M. Akdağ, İ. Bülbül. Design Automation of a Two Scissors Lift. *The European Journal of Research and Development*, 2:178–191, 2022. http://dx.doi.org/10.56038/ejrnd.v2i4.192

[7] H. M. Spackman, *Mathematical Analysis of Scissor Lifts*, 1989. https://dx.doi.org/10.21236/ADA225220

[8] M.N. Kirsanov. Parallelogram mechanism with any number of sections. *Russian Engineering Research*, 38:268–271, 2018. http://dx.doi.org/10.3103/S1068798X18040135
[9] A. T. Dang, D. V. Nguyen, D. N. Nguyen. Applying Parametric Analysis in Enhancing Performance for Double-Layer Scissor Lifts. *Strojniški vest-nik-Journal of Mechanical Engineering*, 69:299–307, 2023. http://dx.doi.org/10.5545/sv-jme.2023.539
[10] A. T. Dang, T. T. N. Nguyen. Investigation on the design of double-stage scissor lifts based on parametric dimension technique. *Machines*, 11:684, 2023. http://dx.doi.org/10.3390/machines11070684
[11] M. Todorović, N. B. Zdravković, M. Savković, G. Marković, G. Pavlović. Optimization of scissor mechanism lifting platform members using HHO method. The 8th International Conference, Transport and Logistics, p. 91–96, 2021.
[12] A. Saxena. Deriving a Generalized, Actuator Position-Independent Expression for the Force Output of a Scissor Lift. arXiv:1611.10182, 2016. https://dx.doi.org/10.48550/arXiv.1611.10182
[13] M. Čuchor, Ľ. Kučera, M. Dzimko. Engineering design of lifting device weighing up to 3.5 tons. *Transportation Research Procedia*, 55:621–628, 2021. http://dx.doi.org/10.1016/j.trpro.2021.07.095
[14] C. Ciupan, E. Ciupan, E. Pop. Algorithm for Designing a Hydraulic Scissor Lifting Platform. In MATEC Web of Conferences; EDP Sciences: Ulis, France, Volume 299, 2019. http://dx.doi.org/10.1051/matecconf/201929903012

Anh-Tuan Dang
Thai Nguyen University of Technology
No. 666, 3/2 Street, Thai Nguyen City, Vietnam
anhtuanck@tnut.edu.vn